Pergamon

Geochimica et Cosmochimica Acta, Vol. 59, No. 12, pp. 2599–2608, 1995

0016-7037/95 $9.50 + .00

0016-7037(95)00152-2

Carbon isotopes of trees from arid environments and implications for reconstructing atmospheric CO_2 concentration

XIAHONG FENG* and SAMUEL EPSTEIN

Division of Geological and Planetary Sciences, 170-25, California Institute of Technology, Pasadena, CA 91125, USA

(*Received September* 2, 1994; *accepted in revised form March* 23, 1995)

Abstract—Four trees from San Dimas, the Santa Monica Mountains and the White Mountains of California, and Sinai Peninsula are studied for carbon isotope ratios. These trees grew in arid environments where vegetation is sparse and canopy effect is minimized. The $\delta^{13}C$ time series obtained from wood segments of these trees contain high-frequency variations and a long-term decreasing trend. The high-frequency signals can be effectively explained by the variations of precipitation. The low-frequency trend cannot be accounted for only by the $\delta^{13}C$ variation of atmospheric CO_2. The CO_2 concentration in the atmosphere also attributed to the progressive depletion in the ^{13}C contents of these trees. These results indicate a possibility of using $\delta^{13}C$ of plants as a proxy indicator of the concentration of atmospheric CO_2, provided that the $\delta^{13}C$ value of the open atmosphere can be constrained independently. Plant water-use efficiency is not a simple function of the CO_2 concentration of the atmosphere. It can increase, remain constant, or decrease with an increase of the atmospheric CO_2 concentration.

INTRODUCTION

The carbon isotopic fractionation associated with the carbon fixation of plants was expressed elegantly by Farquhar et al. (1982). For C3 plants, the carbon isotopic ratio in plant leaves, $\delta^{13}C_{plant}$, is dependent on the carbon isotopic ratio of CO_2 in the ambient air, $\delta^{13}C_{air}$, and the ratio of CO_2 concentration in the intercellular space of leaves, c_i, to that in the atmosphere, c_a, as:

$$\delta^{13}C_{plant} = \delta^{13}C_{air} - a - (b - a)c_i/c_a, \qquad (1)$$

where $\delta^{13}C$ is defined as

$$\delta^{13}C = \left(\frac{(^{13}C/^{12}C)_{sample}}{(^{13}C/^{12}C)_{standard}} - 1\right) \times 1000.$$

The parameter a is the fractionation caused by diffusion of CO_2 from the atmosphere into the intercellular space of leaves, b is the fractionation caused by isotopic discrimination of RuBP carboxylase against $^{13}CO_2$. This simple relationship has been used in a variety of applications to the study of plant physiology (O'Leary, 1988; Farquhar et al., 1989a,b; Ehleringer, 1989; Keeley, 1989; Guy et al., 1989), climate change (Farquhar et al., 1989b; Deleens et al., 1985), and evolution of atmospheric CO_2.

The term $\delta^{13}C_{air}$ on the right side of Eqn. 1 suggests the possibility of using the carbon isotope ratios in plants to reconstruct the history of the $\delta^{13}C$ variations in atmospheric CO_2. Since different sources and sinks of atmospheric CO_2 have distinct isotopic values, the knowledge of the $\delta^{13}C$ values of the atmosphere can contribute to the understanding of the global carbon cycle (Siegenthaler and Joos, 1992).

Attempt to obtain a record of $^{13}C/^{12}C$ variations in atmospheric CO_2 using carbon isotopes in tree rings have been made by a number of authors (Leavitt and Long, 1983, 1989; Stuiver et al., 1984; Krishnamurthy and Epstein, 1990; Epstein and Krishnamurthy, 1990). The technique is encouraged by the observations of a decrease in the $\delta^{13}C$ values of tree rings over the time period from 1800 to the present. This trend correlates with the increase of the CO_2 concentration in the atmosphere and roughly parallels the $\delta^{13}C$ variations of the atmospheric CO_2 measured directly from atmospheric samples (Keeling et al., 1989) and from air bubbles in ice cores (Freidli et al., 1986). However, the observations are not always consistent from tree to tree.

Factors that affect the $\delta^{13}C$ values of tree rings fall into two categories, the climate parameters and the atmosphere parameters. It has been observed that the $^{13}C/^{12}C$ ratios of tree rings correlate with precipitation, humidity, temperature, and light intensity (see review paper by Farquhar et al., 1989a). These factors result in a physiological adjustment of the c_i/c_a ratio and possibly of the value of b in Eqn. 1, and usually cause high-frequency variations in the $\delta^{13}C$ time series of tree rings (see the following results) unless a long-term climate trend occurs.

The most important atmospheric parameter is $\delta^{13}C_{air}$. CO_2 from two major sources is commonly used by plants, CO_2 of the open atmosphere with the $\delta^{13}C$ value of ~ -7 to $-8‰$, and CO_2 recycled or respired by plants and the soil which is much more depleted in ^{13}C ($\sim -20‰$, Keeling, 1958; Park and Epstein, 1960). Therefore, $\delta^{13}C_{air}$ can be affected by the $\delta^{13}C$ value of the open atmosphere, $\delta^{13}C_{atm}$, the density and photosynthetic/respiratory activity of the vegetation, the wind velocity, and the growing stage of a plant (juvenile effect). Assimilation of recycled CO_2 is often referred to as canopy effect, and it can cause both short- and long-term variations in a $\delta^{13}C$ record of tree rings. The effect of wind speed and turbulence are likely to vary seasonally or even daily. Photosynthetic and respiratory activity of a given vegetation is likely to vary with climate, variations of which can be either

* *Present address:* Department of Earth Science, Dartmouth College, Hanover, NH 03755-3571, USA.

short- or long-term. Another example of a long-term trend in $\delta^{13}C$ of tree rings caused by the respired CO_2 is the juvenile effect. Young trees growing under the canopy utilize more respired CO_2, and, therefore, the $\delta^{13}C$ values increase with age during the earliest 20–50 years.

In this article, we discuss the $\delta^{13}C$ records of four trees collected from arid environments, in which the canopy effect is minimized due to sparseness of nearby vegetation. In such environments, the growth rate of a tree is usually limited by availability of moisture, which is indicated by correlations between ring width and precipitation. We will first show that the high-frequency variations in the $\delta^{13}C$ values of these trees can often be effectively explained by the changes in the amount of precipitation. The low-frequency variations (or the trends) are mostly related to the changes in the atmosphere conditions, such as the concentration and $\delta^{13}C$ value of CO_2 in the open atmosphere. Our goal is to obtain the best estimates of the long-term trend from these trees, which is necessary to see how the trend is related to the atmospheric parameters. To do this, we used curve fitting to account for both high- and low-frequency signals simultaneously. The time-dependent terms in the fitted curves are taken as long-term trends of the $\delta^{13}C$ time series.

ANALYTICAL TECHNIQUE

One radial segment of wood is taken from each tree. The bristlecone pine wood was dated by the Tree-Ring Laboratory of the University of Arizona. Other trees are dated by counting annual growth rings under a microscope. Wood samples are further segmented into annual or 5-year sections, ground, and cellulose is extracted from the ground wood. Since these samples were to be measured for both carbon and hydrogen isotopes, cellulose was nitrated into cellulose nitrate using the standard technique (Epstein et al., 1976, 1977; DeNiro, 1981). Cellulose nitrate is oxidized into H_2O and CO_2 by combustion with CuO at 650°C. The $^{13}C/^{12}C$ ratios are determined with a mass spectrometer and expressed as $\delta^{13}C$ values with respect to PDB. The analytical uncertainty is $<0.1‰$ (1σ).

RESULTS

San Dimas Experimental Forest, California, USA

The San Dimas Experimental Forest (SDEF), located in the San Gabriel Mountains northeast of Los Angeles, is a field laboratory for studies in the ecology of chaparral and related ecosystems. Meteorological data are available in various locations in the forest, which was our main consideration for selecting the site. A disc of a Coulter pine (*Pinus coulteri*), which covers the time span of 1946–1992, was collected at Tanbark Flats (34°12′N, 117°45′W, elevation: 2800 m), within 20 m of a meteorological station. This is a fast-growing tree, which allowed isotopic analyses of annual rings.

The SDEF has a Mediterranean-type climate, with mild winters and summer droughts. Most of the precipitation falls from December to March. The total annual precipitation ranges from 256 to 1595 mm with an average of 658 mm (1946–1992). The average annual evaporation potential on the forest is 1630 mm (Dunn et al., 1988). Due to the arid conditions, the growth rate of this tree is determined predominantly by moisture. Since most of the precipitation falls from December to March, we define the hydrological year N to be from October of $N-1$ to September of N. Cross correlations between detrended ring-width and total precipitation of the hydrological year (Fig. 1) show that a significant correlation occurs only when these two variables are in phase (Lag 0). This indicates that the growth rate of the tree is determined by the amount of precipitation during the rainy season immediately prior to the growing season. Thus, a given tree ring in this tree carries little information for the hydrological conditions of any previous years (Lag < 0).

The $\delta^{13}C$ record of the SDEF tree is plotted as a function of time in Fig. 2 (the solid line). The time series contains a decreasing trend on which high-frequency variations are superimposed.

Trees respond to moisture stress by adjusting the stomatal resistance. This results in a change of the intercellular CO_2 concentration, c_i, and hence a change in the $\delta^{13}C$ value of plants according to Eqn. 1. As a result, a correlation between $\delta^{13}C_{plant}$ and precipitation often occurs in plants from arid environments. After the trend of the $\delta^{13}C_{plant}$ time series is removed, $\delta^{13}C$ residuals are systematically related to the total annual precipitation (Fig. 3). The scattered plot in Fig. 3 indicates that the dependency of $\delta^{13}C_{plant}$ on the precipitation may not be linear, it seem to be more sensitive (steeper slope) when the water stress is high and more or less constant when plenty of moisture is available. We note that this observation cannot be generalized. As will be noted later, the relation between the $\delta^{13}C_{plant}$ and precipitation may depend on a number of factors including the climate, the hydrological conditions and the living habits of a tree. There is no significant correlation between the $\delta^{13}C$ of this tree and instrumental temperature.

Our main interest is to quantify the long-term trend and to relate this trend to the evolution of atmospheric CO_2. To obtain the best estimate for the trend, both long- and short-term variations are considered and modelled simultaneously. We assume that, for this tree, the total variation of the $\delta^{13}C_{plant}$ can be explained by two exponential terms, one dealing with the low-frequency signal (the trend) which is a function of time and the other accounts for the high-frequency signal introduced by the interannual variations of precipitation. The equation to be fitted has the following form:

$$\delta^{13}C_{plant} = A_0 + A_1 \exp(A_2(\text{Year} - 1940)) + A_3 \exp(A_4 P), \quad (3)$$

where P is precipitation, and A_0 through A_4 are constants to be determined by regression. The number 1940 in Eqn. 3 is introduced only for numerical convenience. The best fit given by Eqn. 4 is highly significant (p-value < 0.0001), and the modelled and observed $\delta^{13}C_{plant}$ are plotted as a function of time in Fig. 2.

$$\delta^{13}C_{plant} = -21.4 - 1.04 \exp(0.021(\text{Year} - 1940)) + 2.25 \exp(-0.04P). \quad (4)$$

Cheeseboro Canyon, Santa Monica Mountains, California (SMM), USA

The climate pattern of this area is similar to that of SDEF except it is drier due to its relatively low elevation. There is

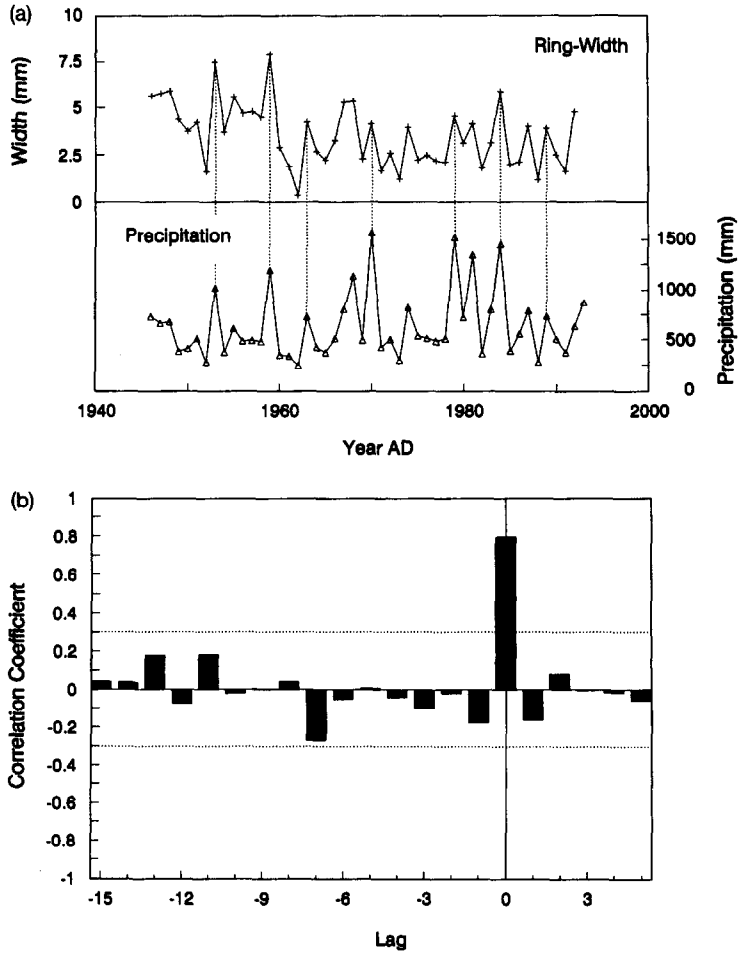

FIG. 1. Correlations between ring-width and precipitation at SDEF. (a) A comparison of time series of ring-width and total hydrological-year precipitation (see text for the definitions of the hydrological year. (b) Cross correlations between ring width and precipitation. The dotted lines are the significant levels at $\alpha = 0.01$. Significant correlation only occurs at Lag = 0.

no meteorological station in the immediate vicinity of the tree, but there are a number of stations within 35 km from the site. None of these stations, except the Los Angeles Weather Station (LAWS), has continuous records longer than fifty years. However, comparisons of the climate records among these stations show coherent variations both in temperature and precipitation, despite the fact that local climate variations are rather complicated in the greater Los Angeles area. The longer time series of the LAWS is used for our discussion. The mean annual temperature recorded at this station is 17.8°C, and the total annual precipitation is 376 mm (1880–1992).

The valley oak (*Quercus lobata*) is one of few native tree species at Cheeseboro Canyon. The oak trees contribute to savanna vegetation and appear scattered over the grassland. Denser clusters of trees are usually found near the bottom of the canyon where supplies of ground water may help them to survive the summer drought. A disc of tree stem was collected from a valley oak at the southern end of Cheeseboro Canyon (34°9′N, 118°44′W, elevation: 350 m). This tree lived from 1775 to 1990, and at the time of its collection it appeared as a single tree with the nearest trees being at least 100 feet away.

The cross-correlation between the ring width and the annual total precipitation (from October 1 to September 30)

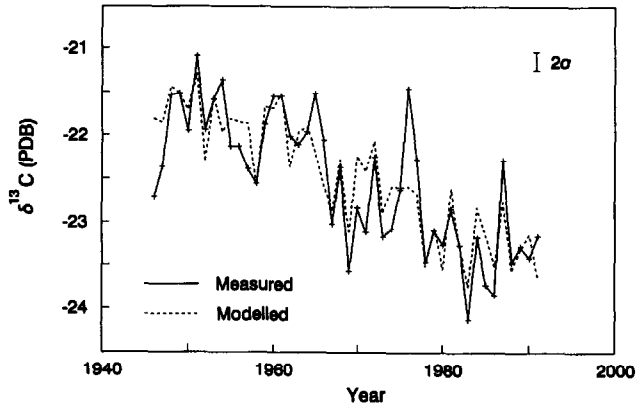

FIG. 2. The $\delta^{13}C$ time series of the Coulter pine at SDEF. The crosses connected by a solid line are the observations, and the dashed line is the model calculations using Eqn. 4.

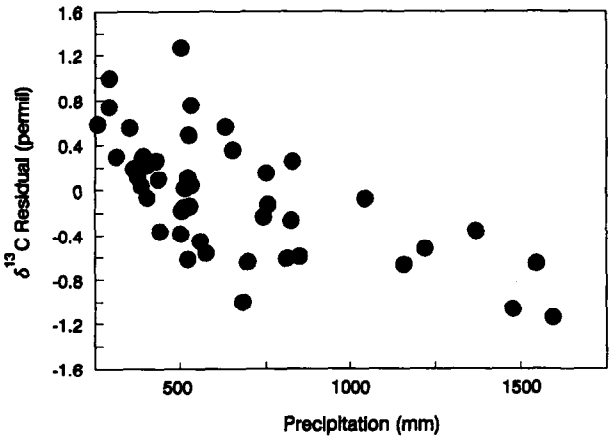

FIG. 3. Scatter plot of the $\delta^{13}C$ residuals of SDEF pine after an exponential trend is removed as a function of precipitation.

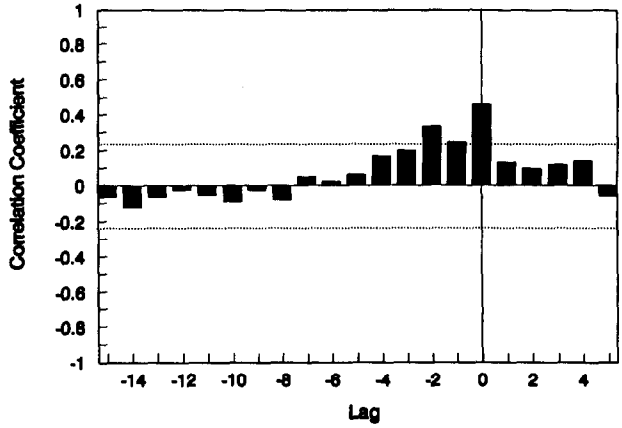

FIG. 4. Cross-correlations between ring-width and precipitation for the valley oak at SMM. The dotted lines are the significant levels at $\alpha = 0.01$. Significant correlation only occurs at Lag = 0, −1, and −2, indicating the precipitation of a given year can affect the rate of tree growth for three years.

shows (Fig. 4) that, unlike the SDEF tree, the growth rate is not only determined by the amount of precipitation of the rainy season immediately prior to the growing season, but also significantly affected by precipitation of the previous two years. This reflects the fact that valley oaks inhabit areas near the supply of ground water which contains a longer hydrologic memory.

To simplify the mathematical treatment, we assume that the growth rate responds on a linear combination of the total precipitation for the past three years. That is,

$$RW_n = X_1P_n + X_2P_{n-1} + X_3P_{n-2}, \quad (5)$$

where RW_n is the detrended ring width for the year n, P_n, P_{n-1}, and P_{n-2} are the total precipitation for the hydrological year n, $n-1$ and $n-2$, and X_1–X_3 are constants to be determined. The multiple regression yielded the following result:

$$RW_n = (3.0P_n + 1.6P_{n-1} + 1.8P_{n-2}) \times 10^{-3}. \quad (6)$$

The regression is highly significant (p-value < 0.0001) and can explain 81% of the total variation in the ring-width data. A three year running average of both measured and modelled ring width values vs. time are plotted in Fig. 5.

The $\delta^{13}C$ and δD values (defined as parts per thousand difference in D/H ratios between a sample and the Standard Mean Ocean Water) of the tree rings were determined for five-year segments and the results are shown in Fig. 6a,b. Similar to the case of SDEF, the $\delta^{13}C$ curve contains a trend and high-frequency fluctuations. The trend has a shape of an exponential function with a rapid decrease in the $\delta^{13}C$ values for the most recent fifty years and much smaller change when going further back in time. After a second order trend of both δD and $\delta^{13}C$ is removed, leaving only the high-frequency signals, a significant correlation is found between the two variables ($r^2 = 0.53$, $n = 43$). Significant correlations also exist between either variable and the five-year ring-width, indicating that precipitation is the common independent variable for the high-frequency variations of all three of these variables. The correlation between δD and precipitation is likely due to the humidity-dependent enrichment of deuterium in leaf water during plant transpiration (e.g., Epstein et al., 1977; Burk and Stuiver, 1981; Edwards and Fritz, 1986; Buhay et al., 1991). We point out, however, that the correlation of high-frequency signals between δD and $\delta^{13}C$ is not commonly observed. In our experience with about twenty trees, δD-$\delta^{13}C$ correlation occurred for only two cases, this tree and the tree of Sinai (to be discussed later). In both locations, the climate is warm and dry.

The precipitation data are not available before 1880; therefore, we used ring-widths as a proxy to model the $\delta^{13}C$ record. A linear relationship between $\delta^{13}C$ and the ring-width is assumed and the curve to be fitted is expressed by the following equation:

$$\delta^{13}C_{plant} = A_0 + A_1RW + A_2 \exp(A_3(\text{MidYear} - 1770)), \quad (7)$$

where RW is the detrended total ring width (mm) of the five-

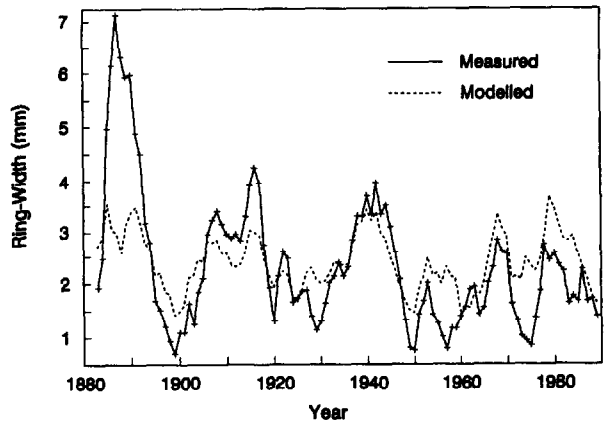

FIG. 5. Measured (solid line) and modelled (dashed line) ring-width time series for the SMM oak. Both time series are smoothed by a 3-year running average.

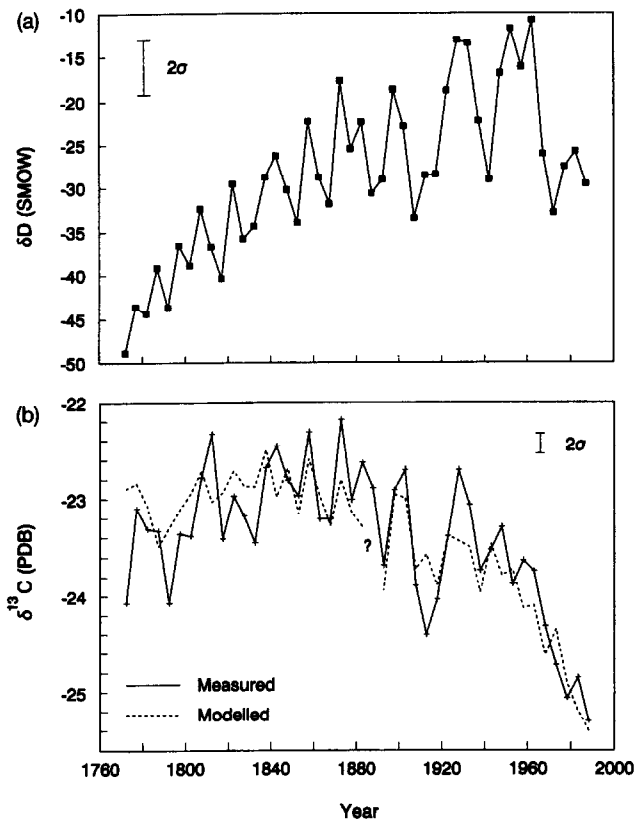

FIG. 6. The δD and δ^{13}C time series of the SMM oak. A significant correlation exists between the high-frequency variations of the δD and δ^{13}C values. The modelled values (dashed line in (b)) are given by Eqn. 8. The question mark in (b) indicates the outlier removed from the model fitting.

year wood segment, and MidYear is the middle year of the segment. One outlier, which corresponds to the exceptionally large value of ring-width for the time interval between 1885 and 1889, was removed from the model calculations. Figure 5 shows that the growth rate for this time period was much higher than the amount of precipitation can account for, and it must reflect other unusual climatic or environmental conditions. The outcome of the curve fitting is given by

$$\delta^{13}C_{plant} = -22.2 - 7.5 \times 10^{-2} RW - 9 \times 10^{-3} \exp(2.6 \times 10^{-2} (\text{MidYear} - 1770)). \quad (8)$$

The modelled results (Fig. 6b), though statistically significant (p-values < 0.0001), are less impressive than those for the previous tree. There are two reasons. First, the ring-width was used as a proxy of precipitation, which added an extra layer of complication and uncertainty. Second, five-year intervals rather than annual rings were analyzed. If one or two rings in a wood segment are particularly wide, they can dominant the overall analysis.

The White Mountains, California, USA

The δ^{13}C records of two old trees, one from the White Mountains of California and the other from Sinai Peninsula were published by Epstein and Krishnamurthy (1990). Based on the striking similarities in the general trend between the two time series, they concluded that both trees had recorded the δ^{13}C values of atmospheric CO_2. In this and the next section, we reexamine these two trees in some detail using the same method developed for the analyses of the two previous cases.

The wood section of the White Mountains was cut from a bristlecone pine (*Pinus longaeva*) collected from the Ancient Bristlecone Pine Forest (37°26′N, 118°10′W, elevation: ~3000 m). Temperature and precipitation were recorded at two weather stations, White Mountain I (~3095 m) and White Mountain II (~3800 m). Between 1956 and 1977, the mean annual temperature and the total annual precipitation were recorded to be 0.9°C and 327 mm at White Mountain I, and −1.7°C and 456 mm at White Mountain II (Powell and Kleiforth, 1991). These readings reflect the general distribution of temperature and precipitation as a function of elevation. The location of the tree is closer to White Mountain I, and it may receive slightly less than 330 mm of precipitation because of its lower elevation.

The cold and dry weather of the White Mountains gives rise to woodland vegetation type rather than a dense forest. The bristlecone pines are commonly distributed in the subalpine from 3050 to 3550 m (Elliott-Fisk and Peterson, 1991). Around the lower treeline, the ring-width was found to be particularly sensitive to precipitation, which is typical of trees near the arid lower forest border (LaMarche, 1974).

Although a significant correlation exists between 5-year ring-width and δ^{13}C of tree rings (both are detrended) ($r^2 = 0.34$ for $n = 90$), the correlation improves considerably between the smoothed versions (fifteen-year running average, Fig. 7) ($r^2 = 0.54$ for $n = 88$). This implies that δ^{13}C of tree rings for this tree responds to climate more strongly in a timescale of one or two decades. The cold and dry climate and the adverse growing conditions in the White Mountains may be the main reasons for this. Bristlecone pine stems are often

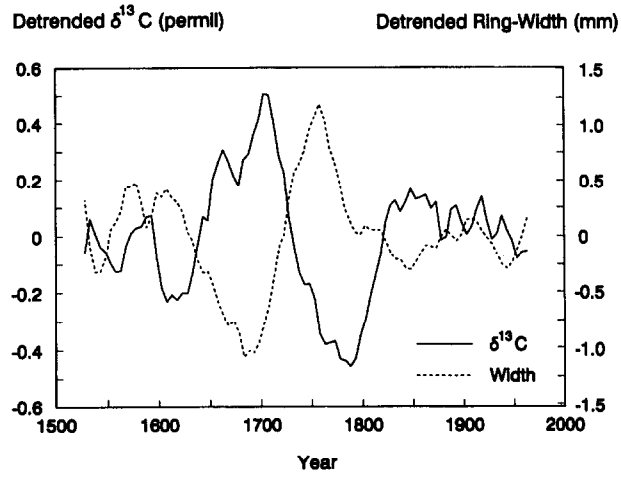

FIG. 7. A comparison of time series of the 5-year ring-width and δ^{13}C for the bristlecone pine. Both time series have been detrended with a second order polynomial function and then smoothed using a 15-year running average.

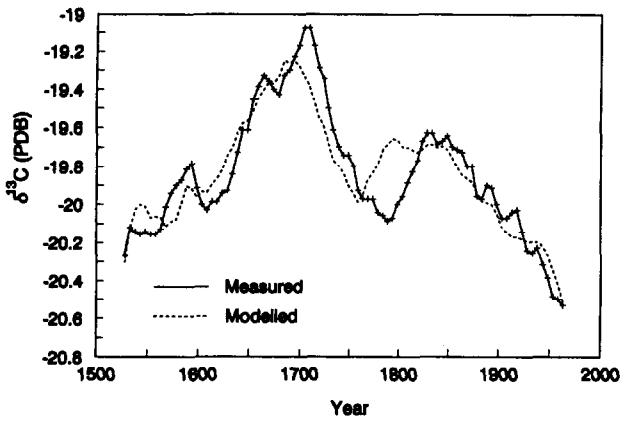

FIG. 8. The measured (solid line) and modelled (dashed line) $\delta^{13}C$ time series for the bristlecone pine. The measured data have been smoothed using a 15-year running average, and the modelled values are calculated using Eqn. 10.

irregular in shape, a growing feature similar to asymmetrical growth (Ramesh et al., 1985) may cause inter-ring variations in ring-width irrelevant to the short-term climate conditions.

In modelling the $\delta^{13}C$ record of the tree, a second-order polynomial trend is assumed, the ring width is used as a proxy indicator of precipitation, and a linear function (suggested by a scattered plot) between the ring width and $\delta^{13}C$ is assumed. To effectively account for the climate signal, the modelling is done on the smoothed time sequence (fifteen-year running average) of the $\delta^{13}C$ values as expressed below:

$$(\delta^{13}C_{plant})_s = A_0 + A_1\,\text{MidYear} + A_2\,\text{MidYear}^2 + A_3 RW_{ds}, \quad (9)$$

where the subscript s stands for smoothed and d for detrended. The modelled results (p-values < 0.001) are given in Eqn. 10, and a comparison of these results with the observations is shown in Fig. 8.

$$(\delta^{13}C_{plant})_s = -66.3 + 5.4 \times 10^{-2}\,\text{MidYear} - 1.6 \times 10^{-5}\,\text{MidYear}^2 - 0.33 RW_{ds}. \quad (10)$$

The reason for the discrepancy between the modelled and measured $\delta^{13}C$ time series during the late 1700s to early 1800s is not clear. It seems to indicate the existence of a nonmoisture dependent signal during this period. The δD record of this tree (Epstein and Yapp, 1976) does not provide any evidence for temperature dependency.

Sinai Peninsula, Egypt

The Sinai tree is a juniper (*Juniperus phoenica*) collected at Gebel Halal, North Sinai (30°40′N, 34°00′E, Elevation: 890 m). In Sinai, *Juniperus phoenica* is one of the very few tree species that has distinct growth rings. The present pattern of the distribution of this species is of a relic nature and they mostly grow along wadi beds. The annual total precipitation is about 100 mm, and the radial growth of *Juniperus phoenica* is shown to be controlled more by water availability than by any other climatic factor (Waisel and Liphschitz, 1968).

The ring-width measurements are not available for this tree. In the case of SMM valley oak, we showed that in an arid environment, the high-frequency variations of δD and $\delta^{13}C$ of a tree correlate with each other, and both variables are related to precipitation. For the Sinai juniper, a significant correlation is also found between the δD (Fig. 9a) and the $\delta^{13}C$ (Fig. 9b, the solid line) records ($r = 0.48$ and $n = 86$) after second-order polynomial trends are removed from both time series. Such high-frequency correlation between δD and $\delta^{13}C$ indicates that both variables respond to climate. As mentioned before, the relationship between the δD and moisture stress is most likely introduced by humidity-dependent fractionation of leaf waters during transpiration. In absence of a more appropriate indicator for precipitation, we use the δD values to remove some of the high-frequency variations due to climate, and assume a linear relationship between $\delta^{13}C$ and δD. If the trend of the $\delta^{13}C$ is to be fitted with a second polynomial function of time, the model to be used here is identical to Eqn. 9 except the variable RW_{ds} is replaced by δD_d as follows:

$$\delta^{13}C_{plant} = A_0 + A_1\,\text{MidYear} + A_2\,\text{MidYear}^2 + A_3\delta D_d, \quad (11)$$

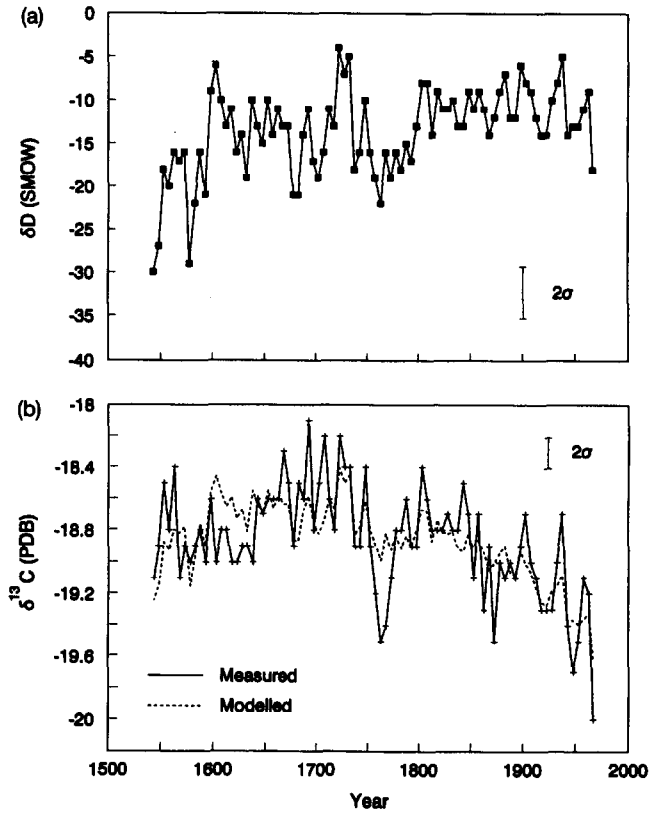

FIG. 9. The δD and $\delta^{13}C$ time series of the juniper tree of Sinai. A significant correlation exists between the high-frequency variations of the δD and $\delta^{13}C$ values. The modelled values (dashed line in (b)) are given by Eqn. 12.

where δD_d is the residual of δD after a second polynomial trend is removed, and A_0 through A_3 are the constants to be determined.

The best fit is given by Eqn. 12 (P-value < 0.0001), and a comparison between measured and modelled $\delta^{13}C$ values is shown in Fig. 9b.

$$\delta^{13}C_{plant} = -49.8 + 3.7 \times 10^{-2}\,\text{MidYear} + 1.1 \times 10^{-5}\,\text{MidYear}^2 + 2.9 \times 10^{-2}\delta D_d. \quad (12)$$

DISCUSSION

A common feature of the four trees we studied is that they all contain a trend and high-frequency variations. These high-frequency variations are predominantly controlled by precipitation, which argues that the contribution of respired CO_2 is not important for these arid environments. Therefore, when we discuss the long-term trends of these records in this section, we will not consider the variations that might be caused by the canopy effect (e.g., Juvenile effect).

We will also assume that the long-term trends seen for these trees do not contain climate signal, namely signal of temperature and precipitation. We provide three arguments to justify this assumption. (1) In the case of SDEF, neither temperature and precipitation contain a long-term trend. This argues that the $\delta^{13}C$ trend of this tree is not related to climate. (2) The precipitation time series from 1880 to 1992 at Los Angeles does not contain a trend, and therefore, the $\delta^{13}C$ trend in SMM tree for this time period is unrelated to precipitation. (3) Although temperature dependency has been reported in a number of studies (Wilson and Grinsted, 1977; Freyer and Belacy, 1983; Stuiver and Braziunas, 1987; Lipp et al., 1991), no significant correlation between $\delta^{13}C$ and temperature exists for high-frequency variations in the case of SDEF and SMM. Therefore, we argue that such correlation would not exist for low-frequency variations either.

The modelled trends of the $\delta^{13}C$ values of the four trees are compared in Fig. 10. The curves are defined by the time-dependent terms in Eqns. 4, 8, 10, and 12, and the constants A_0 are selected such that the $\delta^{13}C$ values equal zero at year 1800 for the three long time-series. For the youngest tree SDEF, the constant A_0 is chosen such that the $\delta^{13}C$ value of the oldest ring (1946) equals the $\delta^{13}C$ value of SMM at 1946.

Direct measurements of the $\delta^{13}C_{atm}$ is available for 1956, 1957 (Keeling, 1958, 1961; Keeling et al., 1989) and between 1978 and 1988 (Keeling et al., 1989). The $\delta^{13}C$ values of CO_2 separated from air bubbles in ice samples provide a $\delta^{13}C_{atm}$ record between 1744 and 1953 (Friedli et al., 1986). These data are plotted in Fig. 10 in a relative scale in which the air analysis of 1956 equals −0.97‰, the average value of the four tree-ring curves at 1956. In the following discussions, $\delta^{13}C_{plant}$ and $\delta^{13}C_{atm}$ are referred to in the relative scale in Fig. 10.

Between 1740 and 1988, the $\delta^{13}C$ curves of tree rings show a decreasing trend similar to that of $\delta^{13}C_{atm}$ in shape, but at a faster rate. For example, from 1956 to 1988, the change in $\delta^{13}C$ of atmospheric CO_2 is −0.83‰, equivalent to a rate of −0.26‰ per decade. For the same time period, the change in

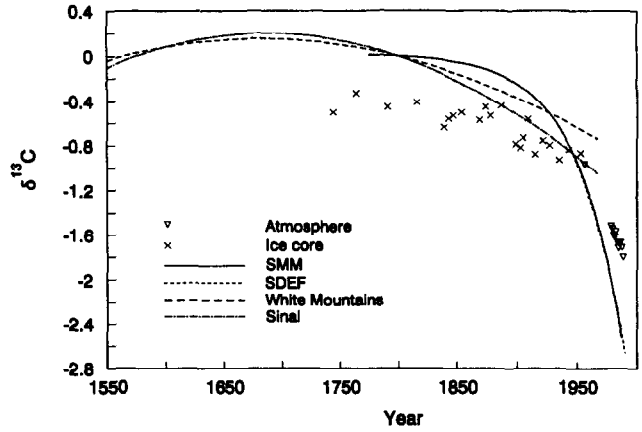

FIG. 10. The trends of the four studied trees. The triangles are the direct measurements of the atmospheric samples, and crosses are the measurements of air bubbles in ice cores. A relative $\delta^{13}C$ scale is chosen to forced the three long series to pass through zero at 1800. For the youngest tree SDEF, the additive constant is determined such that the $\delta^{13}C$ value of the oldest ring (1946) equals the $\delta^{13}C$ values of SMM at 1946. The atmospheric measurements are plotted in a relative scale in which the air analysis of 1956 equals −0.97‰, the average value of the four tree-ring curves at 1956.

$\delta^{13}C_{plant}$, is −1.4‰ for both the Coulter pine of SDEF and the valley oak of SMM. The rate of this change hence is −0.44‰ per decade. This leaves about −0.57‰ change of $\delta^{13}C_{plant}$ unaccounted for by the change of $\delta^{13}C_{atm}$.

It has been shown that C3 plants, growing over a range of CO_2 concentrations characteristic of Last Glacial Maximum to present atmosphere, tend to conserve c_i/c_a ratios (Polley et al., 1993). This may be accomplished by coordination of stomatal and mesophyll functions (Wong et al., 1979) and/or by adjusting the stomatal densities (Woodward, 1987; Van de Water et al., 1994). A slight increase (0.03) in c_i/c_a at CO_2 concentrations from 200 to 350 μmol mol^{-1} has been reported for wheat plants (Polley et al., 1993). A greater increase of 0.09 has been reported for limber pine for change in atmospheric conditions between glacial to Holocene (Van de Water et al., 1994). According to Eqn. 1, every 1‰ decrease in $\delta^{13}C_{plant}$ should correspond to an increase of 0.05 in the c_i/c_a ratio, implying that $\delta^{13}C$ of plants can be a sensitive indicator of the change of c_i/c_a. To see if the CO_2 concentration is related to the unexplained depletion in the trend of $\delta^{13}C_{plant}$, the difference between $\delta^{13}C$ of tree rings and $\delta^{13}C_{atm}$ is plotted as a function of CO_2 concentration (Keeling et al., 1989) (Fig. 11). The average values for all overlapping tree-ring curves at any given time are used to calculate the differences. A highly significant linear relationship ($r^2 = 0.95$) is shown in Fig. 11, which gives a slope of about −0.02‰/ppm. In other words, between 1740 and 1988, $\delta^{13}C_{plant}$ decreased by 0.2‰, and hence, c_i/c_a increased by approximately 0.01 for every 10 ppm increase in the concentration of atmospheric CO_2. This sensitivity is in good agreement with that observed by Van de Water et al. (1994) for limber pine between 18,000 and 11,000 years ago.

The results of this study demonstrate that in the interpretation of the low-frequency trends of $\delta^{13}C_{plant}$ both variations

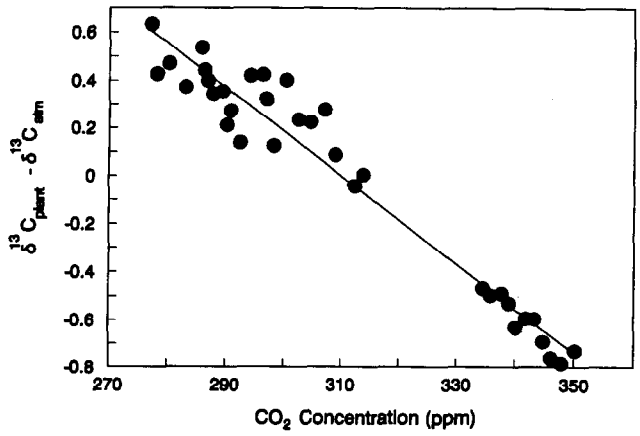

FIG. 11. Plot of the differences between the averaged $\delta^{13}C_{plant}$ and $\delta^{13}C_{atm}$. For a given year for which both $\delta^{13}C_{atm}$ and $[CO_2]$ are available, the $\delta^{13}C_{plant}$ value is the arithmetic mean of the tree-ring curves in Fig. 10 for that year.

of $\delta^{13}C_{atm}$ and c_a have to be considered. However, if the $\delta^{13}C_{atm}$ values can be constrained (for example, by using C4 plants (Marino and McElroy, 1991; Van de Water et al., 1994)), the $\delta^{13}C_{plant}$ may become a potential proxy indicator for the CO_2 concentration in the atmosphere.

We do not know whether various species would respond to the CO_2 concentration to a different degree. These four trees, although all adjusted to the change of the CO_2 concentration in the same direction, may have responded with different sensitivity. The current dataset is not appropriate to provide a quantitative evaluation for the effect of species; therefore, only the averaged sensitivity is given. It is also possible that the effect of species has resulted in some of the earlier observations where the change in the $\delta^{13}C$ of plants more or less matches the decrease in the $\delta^{13}C$ of atmospheric CO_2 (Stuiver et al., 1984; Leavitt and Long, 1989).

Water-use efficiency, W, of C3 species is defined by Farquhar et al. (1989) as the ratio of the net carbon fixed to the total water cost,

$$W = \frac{c_a(1 - c_i/c_a)(1 - \phi_c)}{1.6\nu(1 + \phi_w)}, \qquad (12)$$

where ϕ_c is the proportion of the fixed carbon that is lost (e.g., by respiration), ϕ_w is the unproductive water loss as a proportion of productive water loss, and ν is water vapor pressure difference between the intercellular spaces and the atmosphere. If we allow c_a and c_i/c_a to vary while holding other variables constant, we have

$$dW/W = dc_a/c_a - \frac{d(c_i/c_a)}{(1 - c_i/c_a)}. \qquad (13)$$

The relative change of water-use efficiency is a function of the relative change of c_a and c_i/c_a. For a given change in c_a, the actual response of W depends on the sign and the magnitude of $d(c_i/c_a)$, as well as the magnitude of c_i/c_a. For plants whose c_i/c_a ratios decrease or stay constant with an increasing concentration of atmospheric CO_2, the water-use efficiency increases. In this study, on the other hand, $d(c_i/c_a)$ has the same sign as dc_a, and therefore, the sign of dW/W depends on the relative magnitude of the two terms in Eqn. 13.

Using the value 0.01/10 ppm for $d(c_i/c_a)/c_a$, the possible sign of dW/W as a function of c_a can be illustrated in Fig. 12. For C3 plants, the reported ratios of c_i/c_a vary between 0.60–0.85 (Farquhar et al., 1989a; Polley et al., 1993). Two curves (dotted lines) of $d(c_i/c_a)/(1 - c_i/c_a)$ are calculated as a function of c_a, assuming that the c_i/c_a ratio equals to 0.65 and 0.70, respectively, when c_a equals 280 ppm. The ratio of dc_a/c_a is calculated for 10 ppm increases in c_a, and is plotted as the solid line in Fig. 12. When $dc_a/c_a > d(c_i/c_a)/(1 - c_i/c_a)$, the water-use efficiency increases with c_a. This occurs before the dotted line crosses the solid line. In other words, for low concentrations of atmospheric CO_2, the water-use efficiency tends to increase with increasing c_a. This has two implications. (1) Other things being equal, plant water-use efficiency increases more at high altitudes where the atmospheric CO_2 concentrations are low because of low air pressures. Although an increase of water-use efficiency does not always result in an increase in biomass, it is likely that, in an arid area where water availability is one of the limitations for plant growth, the biomass has increased with an increase of water-use efficiency. Growth increases of conifer stands have been found for trees at high altitudes near the upper treeline, while absent for trees of low altitudes (LaMarche et al., 1984; Graybill and Idso, 1993). The scenario illustrated by Fig. 12 provides one possible explanation for these observations. (2) At least for some plants, water-use efficiency may have increased during the first century after the industrial revolution, but the trend might be reversed in the recent century. This implication may be important for the evaluation of the terrestrial biosphere as a sink of atmospheric CO_2.

CONCLUSION

We have studied carbon isotopes of four trees from arid environments. The rate of tree growth in these environments

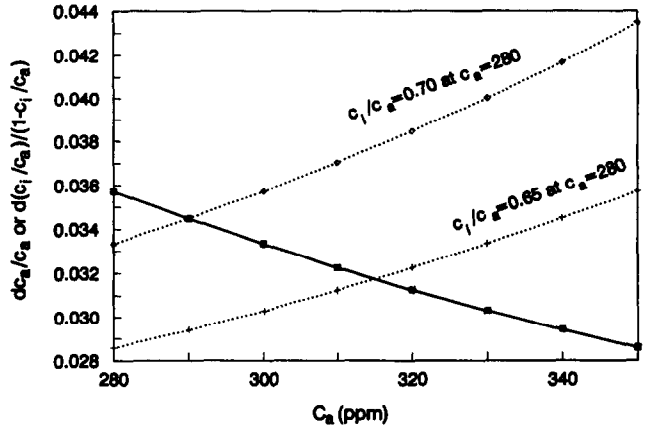

FIG. 12. Values of dc_a/c_a (the solid line) and $d(c_i/c_a)/(1 - c_i/c_a)$ (the dotted lines) plotted as a function of c_a. The calculations of dc_a/c_a are done using 10 ppm as dc_a, and $d(c_i/c_a)/(1 - c_i/c_a)$ are calculated assuming a $d(c_i/c_a)/c_a$ value of 0.01/10 ppm. The plant water-use efficiency increases for the range of c_a where the solid line sits above the dotted line.

is usually limited by precipitation. Depending upon the hydrological conditions and the living habits of a tree species, the precipitation of a given year can affect the rate of growth for one to three years. Because the vegetation is sparse in an arid area, the canopy effect on the $\delta^{13}C$ values of tree rings is minimized. The high-frequency variations of the $\delta^{13}C$ in tree rings can be directly related to the amount of precipitation.

The long-term trends of the $\delta^{13}C$ values in the studied trees contain information about atmospheric CO_2. For the past 250 years, the exponential decrease in the $\delta^{13}C$ values of atmospheric CO_2 is not sufficient to account for the overall decrease of the $\delta^{13}C$ values in the trees. For the four trees we studied, the response of the $\delta^{13}C$ values of tree-rings to the concentration of CO_2 is $-0.02‰$/ppm CO_2.

The plant water-use efficiency is a complicated function of the CO_2 concentration in the atmosphere. For plants that maintain a constant ratio of c_i/c_a or whose c_i/c_a ratios decrease with increasing CO_2 concentration, the water-use efficiency increases. If the c_i/c_a ratio of a plant increase with CO_2 concentration, the water-use efficiency tends to increase when the CO_2 concentration of the atmosphere is relatively low. An increase in biomass may be expected with an increase in water-use efficiency in an arid environment where water availability limits the plant growth.

Acknowledgments—Sample collections at SDEF and SMM were assisted by D. A. Larson, R. M. Rumball-Petre, and R. Sauvajot. The bristlecone pine wood was dated by the Tree-Ring Laboratory of the University of Arizona. Drs. J. Gat and Y. Waisel kindly provided us with climatic and ecological information for Sinai Peninsula. Discussions with J. Bonner and J. Severinghause have been most helpful. We thank E. Dent, X. Xu, and S. McKinnon for their technical support. The manuscript was improved by the comments of T. W. D. Edward and two anonymous reviewers. This work was supported by NSF grant No. ATM9219891 and DOE grant No. DE-FC03-90ER61010.

Editorial handling: H. P. Schwarcz

REFERENCES

Buhay W. M., Edwards T. W. D., and Aravena R. (1991) Fine-tuning the cellulose model for dendroclimatological interpretation: *Proc. Intl. Symp. Use Isot. Techn. Water Resour. Devel., IAEA-SM-319/10P*, Int. Atomic Energy Agency, Vienna, March 1991. pp. 122–123.

Burk R. L. and Stuiver M. (1981) Oxygen isotope ratios in tree cellulose reflect mean annual temperature and humidity. *Science* **211**, 1417–1419.

Deleens E., Treichel I., and O'Leary M. H. (1985) Temperature dependence of carbon isotope fractionation in CAM plants. *Plant. Physiol.* **79**, 202–206.

DeNiro M. J. (1981) The effects of different methods of preparing cellulose nitrate on the determination of the D/H ratios of non-exchangeable hydrogen of cellulose. *Earth Planet. Sci. Lett.* **54**, 177–185.

Dunn P. H. et al. (1988) *The San Dimas Experimental Forest: 50 Years of Research. Pacific Southwest Forest and Range Experiment Station. General Tech. Rep. PSW-104.*

Edwards T. W. D. and Fritz P. (1986) Assessing meteoric water composition and relative humidity from ^{18}O and ^{2}H in wood cellulose: paleoclimatic implications for southern Ontario, Canada. *Appl. Geochem.* **1**, 715–723.

Ehleringer J. R. (1989) Carbon isotope ratios and physiological processes in aridland plants. In *Stable Isotopes in Ecological Research* (ed. R. W. Rundel et al.), pp. 41–54. Ecological Studies 68, Springer-Verlag.

Elliott-Fisk D. L. and Peterson A. M. (1991) Trees. In *Natural History of the White-Inyo Range* (ed. C. A. Hall Jr.), pp. 87–107. Univ. California Press.

Epstein S. and Krishnamurthy R. V. (1990) Environmental information in the isotopic record in trees. *Phil. Trans. Roy. Soc. Lond.* **A330**, 427–439.

Epstein S. and Yapp C. J. (1976) Climatic implications of the D/H ratio of hydrogen in C-H groups in tree cellulose. *Earth Planet. Sci. Lett.* **30**, 252–261.

Epstein S., Yapp C. J., and Hall J. H. (1976) The determination of the D/H ratio of nonexchangeable hydrogen in cellulose extracted from aquatic and land plants. *Earth Planet. Sci. Lett.* **30**, 241–251.

Epstein S., Thompson P., and Yapp C. J. (1977) Oxygen and hydrogen isotopic ratios in plant cellulose. *Science* **198**, 1209–1215.

Farquhar G. D., O'Leary M. H., and Berry J. A. (1982) On the relationship between carbon isotope discrimination and the intercellular carbon dioxide concentration of leaves. *Aust. J. Plant Physiol.* **9**, 121–137.

Farquhar G. D., Hubick K. T., Condon A. G., and Richards R. A. (1989a) Carbon isotope fractionation and plant water-use efficiency. In *Stable Isotopes in Ecological Research* (ed. R. W. Rundel et al.), pp. 21–40. Ecological Studies 68, Springer-Verlag.

Farquhar G. D., Ehleringer J. R., and Hubick K. T. (1989b) Carbon isotope discrimination and photosynthesis. *Annu. Rev. Plant. Physiol. Plant Mol. Biol.* **40**, 503–537.

Freyer H. D. and Balacy N. (1983) $^{13}C/^{12}C$ records in northern hemispheric trees during the past 500 years: Anthropogenic impact and climatic superpositions. *J. Geophys. Res.* **88**, 6844–6852.

Friedli H., Lötscher H., Oeschger H., Seigenthaler U., and Stauffer B. (1986) Ice core record of the $^{13}C/^{12}C$ ratio of atmospheric CO_2 in the past two centuries. *Nature* **324**, 237–238.

Graybill D. A. and Idso S. B. (1993) Detecting the aerial fertilization effect of atmospheric CO_2 enrichment in tree-ring chronologies. *Global Biogeochem. Cycles* **7**, 81–95.

Guy R. D., Warne P. G., and Reid D. M. (1989) Stable carbon isotope ratio as an index of water-use efficiency in C3 holophytes—Possible relationship to strategies for osmotic adjustment. In *Stable Isotopes in Ecological Research* (ed. R. W. Rundel et al.), pp. 55–75. Ecological Studies 68, Springer-Verlag.

Keeley J. E. (1989) Stable carbon isotopes in vernal pool aquatics of differing photosynthetic pathways. In *Stable Isotopes in Ecological Research* (ed. R. W. Rundel et al.), pp. 76–81. Ecological Studies 68, Springer-Verlag.

Keeling C. D. (1958) The concentration and isotopic abundances of atmospheric carbon dioxide in rural areas. *Geochim. Cosmochim. Acta* **13**, 322–334.

Keeling C. D. (1961) The concentration and isotopic abundances of carbon dioxide in rural and marine air. *Geochim. Cosmochim. Acta* **24**, 277–298.

Keeling C. D. et al. (1989) A three-dimensional model of atmospheric CO_2 transport based on observed winds: 1. Analysis of observational data. In *Aspects of Climate Variability in the Pacific and the Western Americas* (ed. D. H. Peterson); *Geophys. Mono. 55*, 165–236.

Keeling C. D., Mook W. G., and Tans P. (1979) Recent trends in the $^{13}C/^{12}C$ ratio of atmospheric carbon dioxide. *Nature* **277**, 121–122.

Krishnamurthy R. V. and Epstein S. (1990) Glacial-interglacial excursion in the concentration of atmospheric CO_2: effect in the $^{13}C/^{12}C$ ratio in wood cellulose. *Tellus* **42B**, 423–434.

LaMarche W. C., Jr. (1974) Paleoclimatic inferences from long tree-ring records. *Science* **183**, 1043–1048.

LaMarche V. C., Jr., Graybill D. A., Fritts H. C., and Rose M. R. (1984) Increasing atmospheric carbon dioxide: Tree ring evidence for growth enhancement in natural vegetation. *Science* **225**, 1019–1021.

Leavitt S. W. and Long A. (1983) An atmospheric $^{13}C/^{12}C$ reconstruction generated through removal of climate effects from tree-ring $^{13}C/^{12}C$ measurements. *Tellus* **35B,** 92–102.

Leavitt S. W. and Long A. (1989) The atmospheric $\delta^{13}C$ record as derived from 56 pinyon trees at 14 sites in the Southwestern United States. *Radiocarbon* **31,** 469–474.

Lipp J. et al. (1991) Stable isotopes in tree ring cellulose and climatic change. *Tellus* **43B,** 322–330.

Marino B. D. and McElroy M. B. (1991) Isotopic composition of atmospheric CO_2 inferred from carbon in C4 plant cellulose. *Nature* **349,** 127–131.

Mook W. G., Koopmans M., Carter A. F., and Keeling C. D. (1983) Seasonal, latitudinal, and secular variations in the abundance and isotopic ratios of atmospheric carbon dioxide 1. Results from the land stations. *J. Geophys. Res.* **88,** 10915–10933.

O'Leary M. H. (1988) Carbon isotopes in photosynthesis. *BioScience* **3,** 328–336.

Park R. and Epstein S. (1960) Carbon isotope fractionation during photosynthesis. *Geochim. Cosmochim. Acta* **21,** 110–120.

Polley H. W., Johnson H. B., Marino B. D., and Mayeux H. S. (1993) Increase in C3 plant water-use efficiency and biomass over Glacial to present CO_2 concentrations. *Nature* **361,** 61–63.

Powell A. M. and Kleiforth D. R. (1991) Weather and climate. In *Natural History of the White-Inyo Range* (ed. C. A. Hall Jr.), pp. 3–27. Univ. California Press.

Ramesh R., Bhattacharya S. K., and Gopalan K. (1985) Dendroclimatological implications of isotope coherence in trees from Kashmir Valley, India. *Nature* **317,** 802–804.

Seigenthaler U. and Joos F. (1992) Use of simple model for studying oceanic tracer distributions and the global carbon cycle. *Tellus* **44B,** 186–207.

Stuiver M. and Braziunas T. F. (1987) Tree cellulose $^{13}C/^{12}C$ isotope ratios and climatic change. *Nature* **328,** 58–60.

Stuiver M., Burk R. L., and Quay P. D. (1984) $^{13}C/^{12}C$ ratios in tree rings and the transfer of biospheric carbon to the atmosphere. *J. Geophys. Res.* **89,** 11,731–11,748.

Van de Water P. K., Leavitt S. W., and Betancourt J. L. (1994) Trends in Stomatal density and $^{13}C/^{12}C$ ratios of *Pinus flexilis* needles during last Glacial-Interglacial cycle. *Science* **264,** 239–243.

Waisel Y. and Liphschitz N. (1968) Dendrochronological studies in Israel II. Juniperus phoenica of north and central Sinai. *La-Yaaran* **18,** 63–67.

Wilson A. T. and Grinsted M. J. (1977) $^{13}C/^{12}C$ in cellulose and lignin as palaeothermometers. *Nature* **265,** 133–135.

Wong S. C., Cowan I. R., and Farquhar G. D. (1979) Stomatal conductance correlates with photosynthetic capacity. *Nature* **282,** 424–426.

Woodward F. I. (1987) Stomatal numbers are sensitive to increases in CO_2 from pre-industrial levels. *Nature* **327,** 617–618.